



A proposal of a new Hartmann or corneal topographer sampling screen geometry

Daniel Malacara-Doblado

Centro de Investigaciones en Optica, A. C.

Loma del Bosque 115. Col. Lomas del Campestre. 37150 Leon, Gto, México

Dedicated to Prof (Dr) Daniel Malacara-Hernández

Hartmann, Hartmann-Shack and many corneal topographers or telescope evaluators measure the shape of human eye corneas or telescope mirrors by finding the slope of the optical surface (or wavefront) at many points over the aperture of a beam of light going out of an optical system. They use an array of sampling points (holes or point light sources). The wavefront or shape of the optical surface under measurement is calculated with an interpolation performing a least squares fitting of the measured data with a set of orthogonal polynomials, typically Zernike polynomials. A problem that remains is that if the wavefront or surface deformations are small and with high slopes, that is, with large transverse aberrations, the Zernike polynomials filter out these small irregularities, smoothing the results more than desired. In this paper, we revise the most common geometry of the sampling arrays and propose a new geometrical configuration with some advantages, and of course, some small disadvantages that have to be taken into account. © Anita Publications. All rights reserved.

doi: [10.54955.AJP.33.12.2024.817-823](https://doi.org/10.54955.AJP.33.12.2024.817-823)

Keywords: Hartmann, Hartmann-Shack, Topographer, Deflectometry, Zernike polynomials.

1 Basic Hartmann and Corneal Topographer Optical Arrangements

The early instrument designed to measure the human cornea deformations was designed by Tscherning [1] and Placido [2] in Portugal (See Fig 1). The examiner observed the cornea of the patient through a small hole in a dark screen with concentric circles engraved or painted over the sampling screen. If the surface of the cornea has deformations with respect to a perfect sphere, the image of the rings will also be deformed. This was a qualitative subjective measurement of the aberrations, sometimes called “deflectometry” and numerous papers had been written to find the aberrations by measuring the distortions of the reflected or refracted pattern.

Twenty-four years later, Hartmann [3,4] invented a similar method to measure the surface deformations of a telescope concave mirror, as shown in Fig 2. An opaque sampling screen with a rectangular array of holes on its surface was placed in contact with the mirror. Then, a point light source was located near the center of curvature of the optical surface under test. An image of the light source is formed near the point light source. If the pupil of the observer’s eye is placed at the image of light source, the illuminated sampling screen with holes is observed. If the optical surface under test has deformations, the illuminated array will not be a regular array of light sources, but it will appear with deformations. As the Placido test, this was a qualitative subjective test, also by measuring slope errors of the surface. A Fresnel lens gives good results in a Hartmann test but the result is a stepped phase, with optical wavefront phase discontinuities.

Corresponding author

e mail: dmalacdo@cio.mx (Daniel Malacara-Doblado)

More than fifty years later, with the advent of image detectors and computers, these methods were greatly improved and made quantitative, more accurate and automatic. Among these modifications was the proposal of the use of a lenticular screen instead of a screen with holes, for using it in a collimated beam of light with a small aperture as reported by Platt and Shack [5]. It is known as Hartmann-Shack test. The applications of the Hartmann scheme is so powerful that it has been used with success in many systems, for example in active optics systems in astronomical telescopes by several researchers, for example, by Wilson *et al* [6].

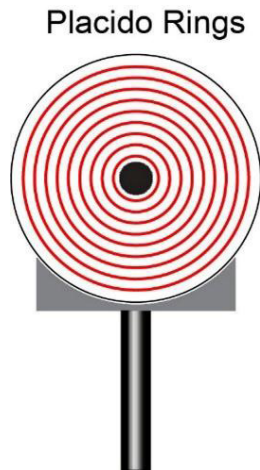


Fig 1. Placido rings to measure the human cornea.

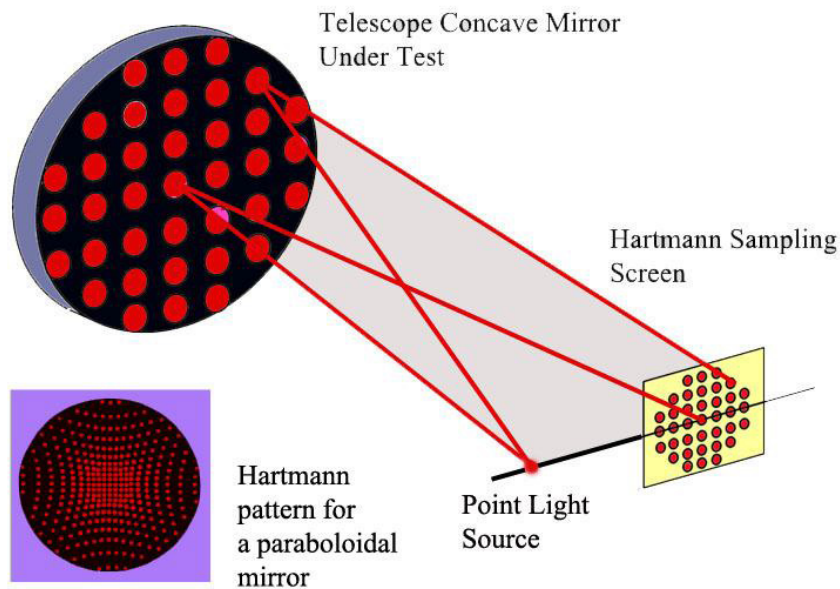


Fig 2. Hartmann test of a concave telescope mirror.

In the past few years, the sampling geometry for the rectangular array of holes or light sources had been modified looking for improvement in the accuracy of the results. In these tests, we measure the transverse aberration of the sampling images produced by each of the sampling places in the wavefront of optical surface being measured. This transverse aberration is the slope of the wavefront (or twice the

slope for reflecting surfaces). The wavefront deformations are twice the surface deformations for the case of mirrors.

The most frequent desired result is the deformations between the ideal perfect optical surface or wavefront and the measured surface. Mathematically, this is obtained by integration of the following expressions:

$$\frac{\partial W(x, y)}{\partial x} = -\frac{TA_x(x, y)}{r - W(x, y)} \approx -\frac{TA_x(x, y)}{r}; \quad \frac{\partial W(x, y)}{\partial y} = -\frac{TA_y(x, y)}{r - W(x, y)} \approx -\frac{TA_y(x, y)}{r} \quad (1)$$

where r is the radius of curvature of the reference spherical wavefront with ideal shape and $W(x, y)$ is the shape of the deformed wavefront with respect to this reference sphere.

The integration to obtain the wavefront deformations is made by one of several possible methods, that can be classified as Modal or Zonal methods. The typical modal method is by polynomial fitting of the measurements to orthogonal polynomials, for example, to Zernike polynomials. A problem with this method is that if the wavefront or surface deformations are small and with high slopes, that is, with large transverse aberrations, the Zernike polynomials filter out these small irregularities, smoothing the results more than desired. In this paper we revise the most common geometry of the sampling arrays and propose a new geometrical configuration. Two examples of surfaces where the polynomial fitting is not appropriate are in Figs 3(a) and 3(b), since the largest surface slope is big and located in a small zone. In this case a zonal integration gives more accurate results. A typical zonal integration is performed by trapezoidal local numerical integration, by small zones, until the whole aperture is covered. However, zonal integration is not yet the best if the sampling points are uniformly and widely spaced. Here, we propose an alternate solution.

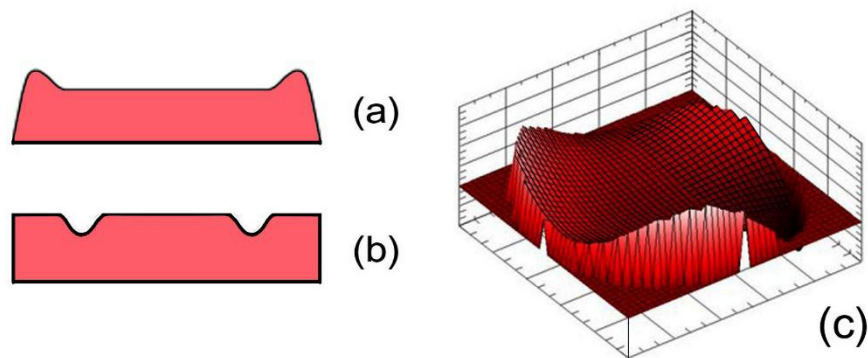


Fig 3. Two surfaces with rotational symmetry (a) and (b), where a polynomial fitting is not the most adequate, and a surface (c) a wavefront where a polynomial fitting works fine.

The measurement of the topography of the human eye cornea was greatly improved by a corneal topographer based on the Placido system using modern techniques to measure the transverse aberrations and integrating these measurements to obtain the corneal deformations. To have the images of the sampling point in a plane, the sampling screen is made concave, with an ovoidal shape, as shown by Mejía Barbosa and Malacara-Hernández [7]. The schematics of a modern corneal topographer is illustrated in Fig 4 [8,9]. The Placido disk is formed by an array of concentric equidistant rings, as illustrated in Fig 4.

Different geometric configurations for the geometric sampling arrays had been tried by Malacara-Doblado and Ghozeil [10]. Some of these configurations will now be reviewed. The most common light array is the one used when testing telescope mirrors with the Hartmann test, using a rectangular array of sampling holes, as illustrated in Fig 5(a). The great advantage of this array is that it is quite simple to construct this sampling screen and that the mathematical discrete integration is quite simple, as described

by Ghozeil and Simmons [11]. However, the main disadvantage is that it does not give the best possible accuracy since it is square and not close to a circular shape as in most optical system pupils.

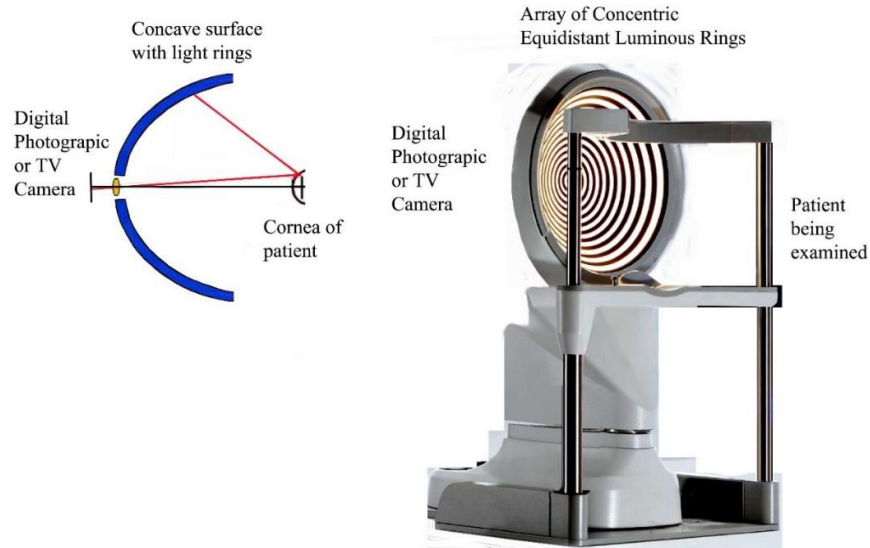


Fig 4. A modern corneal topographer.

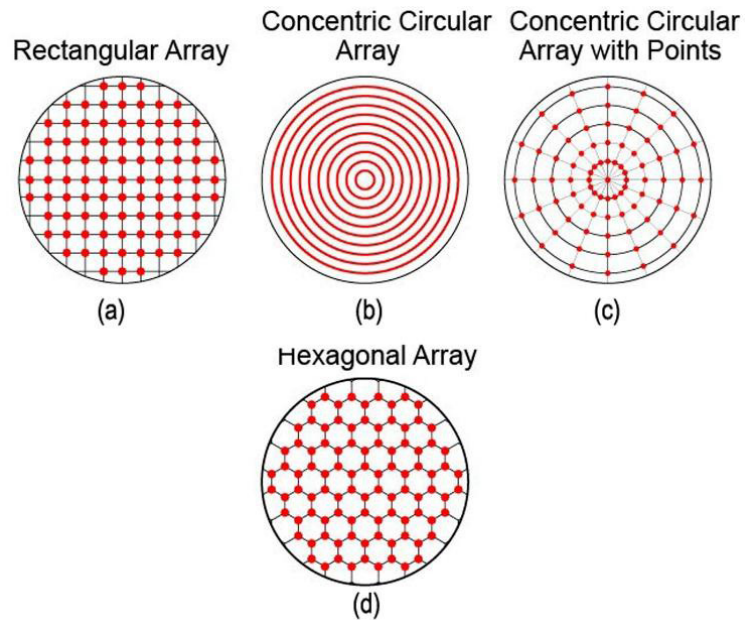


Fig 5. Some common geometries of the Hartmann sampling screens..

The second most common sampling screen is the one with concentric circles, as in the Placido system. It seems logical to think that this type of sampling screen is insensitive to surface slopes (or transverse aberrations) in the tangential directions. However, it has been shown that these errors can be recovered by an iterative procedure, integrating in the radial direction a few times, as demonstrated by Gómez-Tejada *et al* [12].

In some academic projects, other screen configurations with the sampling holes in concentric rings (Fig 5c) and with hexagonal cells (Fig 6d) had been used with different advantages and disadvantages [6].

Frequently, large local surface deformation in optical surfaces and mirrors as well as in human corneas, appear near at the edge of the pupil due to several fabrication factors or produced as a result during a Lasik surgery, or simply because the primary or high order aberrations are large. The result is that the transverse aberrations and hence the spots deviation of the Hartmann pattern near the edge of the pupil are larger. In this case, a polynomial fitting is the proper integration method. This effect produces the need to measure the spots deviation with a local higher sampling density to obtain a better accuracy near the edge of the pupil. Here, we propose some sampling geometries to satisfy this requirement.

2 Analysis of sampling geometries

The analysis of sampling geometries is fundamental for achieving accurate surface measurements in both Hartmann-Shack and corneal topography applications. Traditional methods have been relied on rectangular arrays for simplicity and ease of mathematical treatment, yet these configurations do not always provide the best coverage of the typically circular apertures of optical systems. When measuring the corneal shape or telescope mirrors, it becomes evident that the geometry chosen for the sampling screen can strongly influence the accuracy and sensitivity of the results, particularly near the edge of the pupil where aberrations are often highest.

Recent developments have explored concentric ring arrays, hexagonal cell patterns, and irregularly spaced sampling points to overcome some limitations of traditional arrangements. The use of densified sampling towards the periphery allows for better detection of localized, high-gradient deformations often present after surgical interventions or manufacturing processes. Numerical integration techniques, such as zonal fitting by local trapezoidal integration, offer improvements over classical polynomial fitting, especially in cases where the deformation zones are small and concentrated. This work compares the accuracy of various screen geometries by modeling typical corneal and mirror aberrations. Experimental and simulated data show that adaptive geometric arrangements yield more reliable measurements in regions of high optical slope, where conventional least squares fitting with Zernike polynomials might excessively smooth the actual surface topography. Ultimately, optimizing the sampling scheme enhances not only the reliability of deformation detection but also the repeatability and robustness of the diagnostic or testing method.

3 New geometrical configuration of arrays of sampling points

To satisfy the requirements of a screen configuration like those as in Fig 6 may be implemented. This screen can have any number N of concentric rings given by.

$$s = \frac{D}{(N+2)(N+1)} \quad (2)$$

where $D = 8$ mm is the diameter of the eye in the pupil plane covered by the sampling screen and s is a distance along the radial direction, as shown in Fig 7. The first ring has a semi-diameter given by $(N+1)s$. Each of the subsequent outer rings n have a semi-diameter, greater than the previous smaller ring by an amount $(N-n+1)s$.

The sampling points can be eliminated to use continuous rings as in Fig 7. The sensitivity to angular errors is not lost, as shown by Gómez-Tejada *et al* [12]. The more convenient of these sampling screens one that has the maximum density of sampling points but these high density points are clearly separated in the images of the measured sampling spots. Then, the results are least squares fitted to Zernike polynomials and then integrated to obtain the surface deformations.

The most convenient Zernike polynomials to perform the least squares fitting are those ordered by the value of the sum of degree n of the radial components plus the angular azimuthal power l of

the angular components. These are the Zernike polynomials, commonly recognized as the Arizona Fringe Polynomials. Note these polynomials are no longer an orthonormal set of polynomials and the coefficients give Peak-to-valley or rms values for the aberration coefficients. The earliest antecedent of this system of Zernike polynomials was described by Creath and Parks [12] and Gross [13,14]. There are several advantages of this ordering. One of them is that when the series is truncated at a certain value of $n + l$, the last polynomial will be a spherical polynomial term, with the same value of n but higher value of $n + l$.

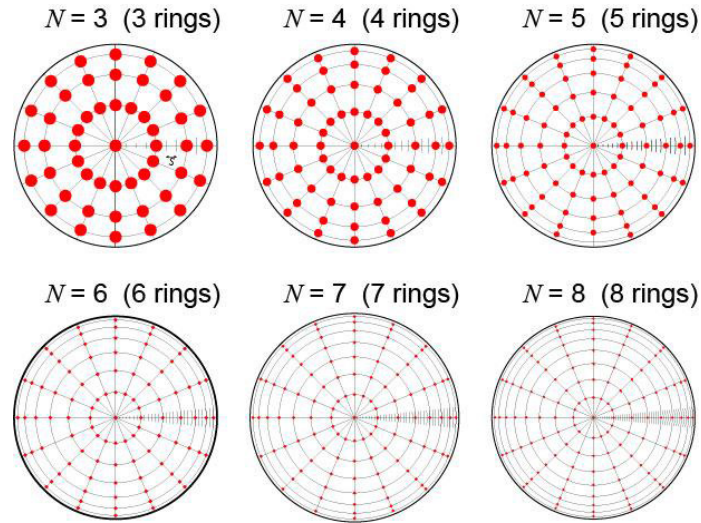


Fig 6. Some new sampling screens with sampling points.

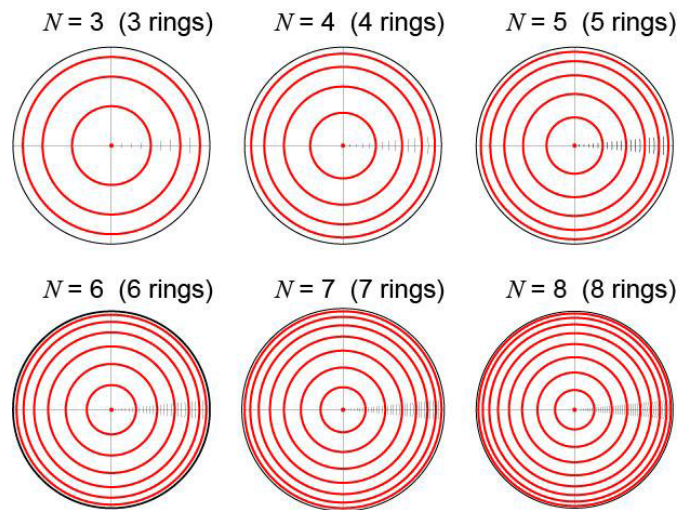


Fig 7. Sampling screens with continuous rings with on unequal separations.

The adequate sampling screen is one that has the maximum density of sampling points but these high density points are clearly separated in the plane of the measured images of the sampling spots. Then, the results are least squares fitted to Zernike polynomials and then integrated to obtain the surface deformations.

4 Conclusions

We have revised the most important characteristics of some traditional and new geometries for the sampling screens. One is that the accuracy sensitivity is greater at the edge than at the center of the pupils due to their smaller separations. This variable frequency of the rings is common with the Fresnel Zone plate, but it is not the same. The area of each cell with four points in the screen is the same at all places. Thus, the sampling points density is uniform over the whole aperture.

If the wavefront or surface deformations are small and with high slopes, that is, with large transverse aberrations, the Zernike polynomials filter out these small irregularities, smoothing the results more than desired. In this paper, we have revised the most common geometry of the sampling arrays and have proposed a new geometrical configuration in order to solve this problem.

References

1. Tscherning M, Die Monochrotischen Aberrationen des Menschlichen Auges, *Z Psychol Physiol Sinn*, 6(1894)456–471.
2. Placido A, Novo Instrumento de Exploração da Córnea, *Periodico d'Óftalmologica*, 5(1880)27–30.
3. Hartmann J, Objektivuntersuchungen, *Zt Instrumentenk*, 24(1904)33.
4. Hartmann J, Objektivuntersuchungen, *Zt Instrumentenk*, 97(1904)97.
5. Platt B C, Shack R, Lenticular Hartmann Screen, *Opt Sci Newsl*, 5(1971)15.
6. Wilson R N, Franza F, Noethe L, A System for Optimizing the Optical Quality and Reducing the Costs of Large Telescopes, *J Mod Opt*, 34(1987)485–509.
7. Mejía-Barbosa Y, Malacara-Hernández D, Object surface for applying a modified Hartmann Test to measure Corneal Topography, *Appl Opt*, 40(2001)5778–5786.
8. Henson D B, *Optometric Instrumentation*, 2nd Edn, Chapter 5, (Keratometers, Butterworth Heinemann, Oxford), 1996.
9. Corbett M, O'Brart D, Rosen E, Stevenson R, *Corneal Topography: Principles and Applications*, 2nd edn, (Springer), 2019.
10. Malacara-Doblado D, Ghozeil I, Hartmann, Hartmann-Shack and Other Screen Tests, Chapter 10 in Malacara D, *Optical Shop Testing*, 3rd Edn, (Wiley Interscience, New York), 2007.
11. Ghozeil I, Simmons J E, Screen Test for Large Mirrors, *Appl Opt*, 13(1974)1773–1777.
12. Gómez-Tejada D, Malacara-Hernández Z, Malacara-Doblado D, Malacara-Hernández D, Zonal Integration of Circular Hartmann and Placido Patterns with Non-Rotationally Symmetric Aberrations, *J Opt Soc Am A*, 37(2020)1381–1389.
13. Creath K, Parks R E, Optical Metrology at the Optical Sciences Center: A Historical Review, *Proc SPIE*, 91860T (2014); doi.org/10.1117/12.2064376.
14. Gross H, *Handbook of Optical Systems*, Vol 1, Fundamentals of Technical Optics, (Wiley-VCH), p 501, 2005.
15. Gross H, *Handbook of Optical Systems*, Vol 2, Physical Image Formation, (Wiley-VCH), p 212, 2005.

[Received: 30.11.24; rev recd: 25.12.2024; accepted: 30.12.2024]